UC Irvine
UC Irvine Previously Published Works

Title

Differential involvement of hippocampal subfields in the relationship between Alzheimer's pathology and memory interference in older adults

Permalink

https://escholarship.org/uc/item/3kc9s9qt

Journal

Alzheimer's & Dementia Diagnosis Assessment & Disease Monitoring, 15(2)

ISSN

2352-8729

Authors

Adams, Jenna N
Márquez, Freddie
Larson, Myra S
et al.

Publication Date

2023-04-01

DOI

10.1002/dad2.12419

Peer reviewed

RESEARCH ARTICLE

Differential involvement of hippocampal subfields in the relationship between Alzheimer's pathology and memory interference in older adults

Jenna N. Adams[1] | Freddie Márquez[1] | Myra S. Larson[1] | John T. Janecek[1] | Blake A. Miranda[1] | Jessica A. Noche[1] | Lisa Taylor[2] | Martina K. Hollearn[1] | Liv McMillan[1] | David B. Keator[2] | Elizabeth Head[3,4,5] | Robert A. Rissman[6,7] | Michael A. Yassa[1]

[1]Department of Neurobiology and Behavior and Center for the Neurobiology of Learning and Memory, University of California, Irvine, California, USA

[2]Department of Psychiatry and Human Behavior, University of California, Irvine, California, USA

[3]Department of Pathology and Laboratory Medicine, University of California, Irvine, California, USA

[4]Department of Neurology, University of California, Irvine, California, USA

[5]Department of Neurology, University of Kentucky, Lexington, Kentucky, USA

[6]Department of Neurosciences, University of California, San Diego, California, USA

[7]Veterans Affairs San Diego Healthcare System, San Diego, California, USA

Correspondence
Jenna N. Adams and Michael A. Yassa, 1418 Biological Sciences 3, Irvine, CA 92697-3800, USA.
Email: jnadams@uci.edu; myassa@uci.edu

Abstract

Introduction: We tested whether Alzheimer's disease (AD) pathology predicts memory deficits in non-demented older adults through its effects on medial temporal lobe (MTL) subregional volume.

Methods: Thirty-two, non-demented older adults with cerebrospinal fluid (CSF) (amyloid-beta [$A\beta_{42}$]/$A\beta_{40}$, phosphorylated tau [p-tau]$_{181}$, total tau [t-tau]), positron emission tomography (PET; 18F-florbetapir), high-resolution structural magnetic resonance imaging (MRI), and neuropsychological assessment were analyzed. We examined relationships between biomarkers and a highly granular measure of memory consolidation, retroactive interference (RI).

Results: Biomarkers of AD pathology were related to RI. Dentate gyrus (DG) and CA3 volume were uniquely associated with RI, whereas CA1 and BA35 volume were related to both RI and overall memory recall. AD pathology was associated with reduced BA35, CA1, and subiculum volume. DG volume and $A\beta$ were independently associated with RI, whereas CA1 volume mediated the relationship between AD pathology and RI.

Discussion: Integrity of distinct hippocampal subfields demonstrate differential relationships with pathology and memory function, indicating specificity in vulnerability and contribution to different memory processes.

KEYWORDS
Alzheimer's disease, amyloid-beta, medial temporal lobe, memory, neurodegeneration, tau

1 | BACKGROUND

The mechanisms leading to memory decline in both healthy aging and the earliest stages of preclinical Alzheimer's disease (AD) are still not well understood. Two possible factors may lead to memory impairment in older adults: the accumulation of AD pathology and neurodegeneration within the medial temporal lobe (MTL), which supports memory processing. How pathology and MTL neurodegeneration impact different aspects of episodic memory loss (e.g., forgetting vs interference) has not been tested comprehensively.

Protein aggregates comprising amyloid-beta (Aβ; i.e., amyloid plaques) and hyperphosphorylated tau (i.e., neurofibrillary tangles) are hallmark features of AD and begin to accumulate 10–20 years before clinical symptom onset.[1–3] Currently the predominant and best-established modalities for assessing Aβ and tau pathologies in vivo are measuring concentrations within cerebrospinal fluid (CSF) and visualizing deposition with positron emission tomography (PET).[4–6] Previous studies have shown strong relationships between AD pathology and memory, particularly with tau pathology, in cognitively normal samples.[7,8]

In addition to pathological protein aggregation, neurodegeneration of specific subregions within the MTL may strongly contribute to early memory decline. Specifically, the entorhinal cortex and hippocampus are critical to both the formation and recollection of memories.[9] Although various factors may lead to neurodegeneration, AD pathology strongly contributes to MTL neurodegeneration in older adults, with specific subregions such as entorhinal cortex, CA1, and subiculum being more vulnerable to pathology.[10–16] Because different aspects of episodic memory may preferentially engage distinct MTL subregions, the difference in vulnerability to pathology may determine which memory domains first exhibit impairment.

The goal of the current study was to examine the pathological mechanisms that lead to initial memory deficits in preclinical AD. We hypothesized that the accumulation of AD pathology is associated with subtle episodic memory deficits in particular domains, in part through its effects on MTL volume. We tested this hypothesis in a sample of non-demented older adults who have both PET and CSF biomarkers of AD pathology, high-resolution structural magnetic resonance imaging (MRI) to assess MTL subregional volumes, and neuropsychological assessment to measure subtle deficits in episodic memory.

Specifically, we tested the hypothesis that retroactive interference (RI), a more granular measure of memory reflecting the resistance to interference during consolidation,[17] would be a sensitive marker of hippocampal integrity[18–20] and AD pathology. While deficits in traditional episodic memory tasks such as delayed recall performance may reflect non-specific mechanisms of forgetting, RI isolates the interference of new information upon previously encoded information.[17] This process has been proposed to involve pattern separation-like mechanisms,[21] performed in dentate gyrus (DG) and CA3,[22] as well as the involvement of cellular competition mechanisms in dorsal CA1 during consolidation.[20]

First, because the factors associated with deficits in RI in older adults have not been characterized extensively, we established

RESEARCH IN CONTEXT

1. **Systematic Review**: Prior literature was reviewed by searching Google Scholar, PubMed, and identifying relevant references in these publications.
2. **Interpretation**: Our focus on a more granular measure of memory consolidation—retroactive interference, a hippocampal dependent process that reflects resistance to interfering information during consolidation—revealed strong relationships with Alzheimer's disease (AD) pathology and hippocampal subfield volume. We demonstrate that the relationship between AD pathology and retroactive interference is mediated by CA1 volume, whereas the relationship between dentate gyrus (DG) volume and retroactive interference is independent of AD pathology.
3. **Future Directions**: Our findings suggest that retroactive interference may be a more sensitive behavioral biomarker of subtle memory impairment than delayed recall, reflecting both AD pathology and hippocampal integrity. Furthermore, because CA1 volume links developing pathology to early memory impairment, CA1 volume may be a valuable neurodegenerative marker in the preclinical phase of AD.

whether specific MTL subregions and AD pathologies were related to RI performance. Because DG is resistant to the effects of AD pathology until late in AD, whereas CA1 is an early target of pathology,[2] we then performed a series of analyses to measure unique and shared contributions of AD pathology and DG/CA1 volume to RI performance. Finally, we constructed mediation models to test whether AD pathology exerts effects on RI through reduced volume of CA1.

2 | METHODS

2.1 | Participants

Participants were recruited from the Alzheimer's Disease Research Center (ADRC) Longitudinal Cohort and the Biomarker Exploration in Aging, Cognition, and Neurodegeneration (BEACoN) Study at the University of California, Irvine. Participants were included if they were cognitively normal (Clinical Dementia Rating [CDR] = 0) and received both [18]florbetapir-PET and CSF measures of AD pathology. Participants gave written informed consent in accordance with the institutional review board of the University of California, Irvine, and were compensated for their participation.

2.2 | Neuropsychological assessment

Participants completed neuropsychological assessments including the Mini-Mental State Exam (MMSE)[23] and the Rey Auditory Verbal Learning Test (RAVLT).[24] The RAVLT is a word list learning task that assesses immediate and delayed memory. We analyzed: (1) RI, which compares memory for the target list of words before (A5) and after (A6) a distractor list is presented (A6/A5; lower scores indicate more interference), and (2) *delayed recall* (DR), which tests free recall for the target list of words after a 20-min delay from the last learning trial.

2.3 | CSF acquisition and processing

CSF was obtained from participants via lumbar puncture, performed with standard clinical research methods in an aseptic fashion by a board-certified neurologist. CSF was collected in a 15 mL Falcon tube, placed on ice until processed (within 2 h), aliquoted into 250 μL volumes, and stored at $-80°C$ until use. $A\beta_{42}$, $A\beta_{40}$, p-tau$_{181}$, and total tau (t-tau) were quantified on the Lumipulse G 1200 automated platform using a chemiluminescent enzyme immunoassay (CLEIA) by the UCSD Shirley-Marcos ADRC Biomarker Core. A cutoff of 0.062 was used to determine $A\beta_{42}/A\beta_{40}$ positivity.[25]

2.4 | PET acquisition and processing

Participants received ^{18}F-florbetapir-PET (FBP) to quantify $A\beta$ on an ECAT High Resolution Research Tomograph (HRRT, CTI/Siemens, Knoxville, TN, USA); 10 mCi of tracer was injected, and four, 5-min frames were collected from 50 to 70 min post-injection. Data were reconstructed with attenuation correction, scatter correction, and 2 mm^3 Gaussian smoothing. Data were realigned, coregistered to the structural MRI, and normalized by a whole cerebellum reference region to produce standardized uptake value ratio (SUVR) images. Additional smoothing was applied to achieve an effective resolution of 8 mm^3. The mean SUVR of a previously validated cortical composite region was quantified (FBP SUVR) and used to determine $A\beta$-PET positivity using a threshold of > 1.11 SUVR.[26,27]

2.5 | Structural MRI

Participants underwent structural MRI on a 3T Prisma scanner (Siemens Medical System) equipped with a 32-channel head coil. Whole-brain high-resolution T1-weighted volumetric magnetization prepared rapid gradient echo (MPRAGE) images (repetition time/echo time [TR/TE] = 2300/2.38 ms, flip angle = 8°, 0.8 mm^3 resolution, 240 slices) and high-resolution three dimensional (3D) T2-weighted turbo spin echo (TSE) images (oblique coronal orientation, 0.4 × 0.4 mm in-plane resolution, 2 mm slice thickness, TR/TE = 5000/84 ms, 23 slices) were acquired. Structural MR images were processed through FreeSurfer v.6.0[28] to obtain cortical native-space regions of interest

for FBP quantification. To obtain measures of MTL subregional volumes (entorhinal cortex, BA35, DG, CA3, CA1, subiculum), T1 and T2 images were processed with Automated Segmentation of Hippocampal Subfield (ASHS) software.[29] The resulting segmentations were visually quality checked by trained raters for mislabeling, and all passed inspection. Volumes of each region were normalized by total intracranial volume estimates derived from advanced normalization tools (ANTs).[30]

2.6 | Assessing concordance between PET and CSF

To further establish validity of the automated Lumipulse assay for CSF analyses in cognitively normal older adults,[31] we assessed relationships between FBP-PET and CSF biomarkers (Figure S1; Supplementary Methods). FBP SUVR was significantly correlated with CSF $A\beta_{42}/A\beta_{40}$ and p-tau (p's < 0.05), but not t-tau (Figure S1A-C). $A\beta$ positivity was highly concordant when applying validated thresholds to FBP SUVR and CSF $A\beta_{42}/A\beta_{40}$ (30/32, 93.8% concordance; Figure S1D), and CSF $A\beta_{42}/A\beta_{40}$ robustly predicted $A\beta$-PET status (Figure S1E). Due to the consistency of these results with previous findings in mixed memory cohorts[25,32,33] and healthy older adults,[31] we subsequently analyzed both PET and CSF biomarkers of AD pathology in relation to memory and MTL volumes.

2.7 | Statistical analysis

Statistical analyses were performed using Jamovi v1.6 and RStudio v1.4. Partial correlations relating biomarkers, memory, and MTL subregional volume covaried for age, sex, and education, and CSF-memory interval where appropriate. One participant's p-tau and t-tau levels were a significant outlier (>2 SD of sample mean) and removed from analyses involving these measures. The strength of correlations was statistically compared using a Steiger z-test.[34]

Stepwise linear regression models predicting to RI were constructed with demographic variables in the first step (age, sex, education), FBP SUVR in the second step, and volume (either CA1 volume or DG volume) in the third step.

To quantify proportional shared effects of our major correlated predictors (CA1 volume, DG volume, FBP SUVR), we performed commonality analyses.[35] Analyses were performed in RStudio using the "yhat" package, which conducts commonality analyses based upon all-possible-subsets regression. Separate models were constructed to predict to RI and delayed recall. Effects of covariates (age, sex, and education) were regressed out prior to analysis. The first analysis included CA1 and DG volume, whereas the second included CA1 volume, DG volume, and FBP SUVR.

Mediation analyses were performed in RStudio using the "mediation" package.[36] Linear models were first constructed to test the effect of the independent variable (IV) on the mediator (mediator ~ IV + covariates) and to test for the effect of both the IV and mediator on the dependent variable (DV) simultaneously (DV ~ IV + mediator +

TABLE 1 Demographics and summary measures of the sample.

Demographics	M (SD) or N (%)
Age (years)	73.5 (4.72)
Sex (female)	24 (75%)
Education (years)	16.4 (2.42)
MMSE	28.2 (1.59)
APOE ε4+[a]	12 (38.7%)
CSF $A\beta_{42}/A\beta_{40}$	0.069 (0.23)
CSF p-tau$_{181}$ (pg/mL)	42.4 (20.10)
CSF t-tau (pg/mL)	307 (128.00)
FBP SUVR	1.14 (0.18)
Time between CSF-PET (years)	0.92 (0.82)

Abbreviations: Aβ, amyloid beta; APOE, apolipoprotein E; CSF, cerebrospinal fluid; FBP, ^{18}F-florbetapir PET (positron emission tomography); MMSE, Mini-Mental State Exam; p-tau, phosphorylated tau$_{181}$; SUVR, standardized uptake value ratio; t-tau, total tau.

[a]One participant missing APOE genotype.

FIGURE 1 Relationships between memory, Alzheimer's pathology, and medial temporal lobe (MTL) volume. Correlation matrix represents partial correlation Pearson's *r* values, controlling for age, sex, and education (and CSF time interval where appropriate). Strong relationships were found between RI with pathology and MTL volume, especially DG and CA1. Alzheimer's pathology was most closely associated with BA35 (transentorhinal cortex), CA1, and Sub (subiculum) volume. See Table S1 for exact *r* and *p*-values of each correlation. CSF, cerebrospinal fluid; DG, dentate gyrus; DR, delayed recall; EC, entorhinal cortex; FBP SUVR, 18F-florbetapir-PET; MTL, medial temporal lobe; p-tau, phosphorylated tau$_{181}$; RI, retroactive interference; t-tau, total tau. ***$p < 0.001$ **$p < 0.01$ *$p < 0.05$ $^{+}p < 0.10$.

covariates). Each linear model included age, sex, and education as covariates of no interest. The mediation models assessing CSF p-tau additionally included the time delay between CSF and memory assessment/MRI as a covariate in both linear models. These models were then inputted into the "mediate" function. Models were simulated 10,000 times using the quasi-Bayesian Monte Carlo method to produce confidence intervals (CIs) and considered significant if the CI for the Average Causal Mediation Effects (ACME) term did not cross zero. Alternative models were performed by predicting to delayed recall instead of RI, and by testing alternative regions to determine the specificity of CA1 in the mediated effect.
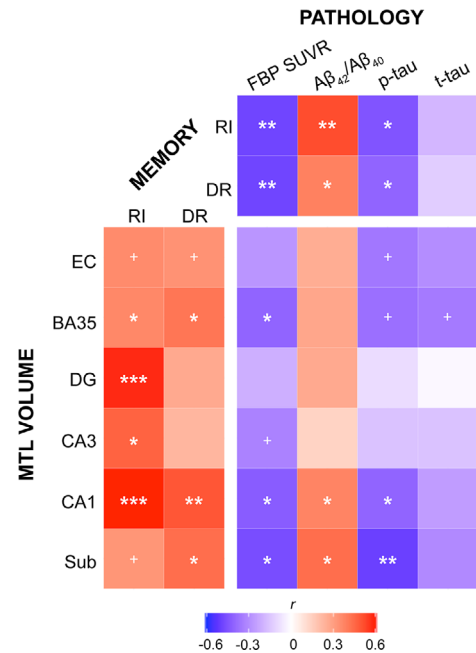
3 | RESULTS

3.1 | Demographics

Thirty-two cognitively normal older adults received neuropsychological assessment, both FBP-PET and CSF, and structural MRI, and were included in the present analysis. Full demographic information of the sample is presented in Table 1. Participants were 73.5 years old on average (range 64–86 years), predominantly female (75%), and received CSF and PET within an average of 0.92 years.

3.2 | Episodic memory measures are associated with AD pathology and MTL subregional volume

We first assessed the relationship between episodic memory, AD pathology measured with PET and CSF, and MTL subregional volumes (Figure 1). Our primary memory outcome measure was RI, a hippocampal dependent process[18–20] that reflects resistance to interfering information during consolidation.[17] As a secondary measure, we

also investigated DR, a more traditional outcome measure that reflects non-specific mechanisms of forgetting. RI and DR were moderately correlated within our sample ($r = 0.64, p < 0.001$).

RI and DR had similar associations with AD pathology. Worse performance on both RI and DR was associated with higher FBP SUVR (RI: $r = -0.49, p = 0.006$), lower CSF $A\beta_{42}/A\beta_{40}$ (RI: $r = 0.52, p = 0.005$), and higher p-tau pathology (RI: $r = -0.45, p = 0.02$; Figure 1; see Table S1 for DR statistics). There was no association between RI or DR with t-tau (p's > 0.35), indicating the specificity of both measures to AD-specific pathology.

We then assessed the relationship between memory and subregional MTL volumes (Figure 1), including measures of the entorhinal cortex (EC), transentorhinal cortex (BA35), and hippocampal subfields (dentate gyrus, DG; CA3, CA1, subiculum). RI was positively correlated with volume in nearly all regions—most strongly with CA1 ($r = 0.61$, $p < 0.001$) and DG ($r = 0.58, p < 0.001$), but also with CA3 and BA35 (p's < 0.05, Table S1), and a trend-level relationship with EC and subiculum (0.05 < p's < 0.10, Table S1). In contrast, DR was positively associated with volume in CA1, subiculum, and BA35, with a trend in EC (see Table S1 for statistics). There was no relationship between DR and DG or CA3 volume (p's > 0.16).

Due to strong correlations ($p < 0.001$) found between both DG and CA1 with RI, and a non-significant correlation between DG volume and DR, we next formally tested whether these associations were stronger with RI than with DR. The correlation between DG volume and RI was significantly stronger than that between DG volume and DR ($z = 2.30$, $p = 0.02$, Steiger z-test). In contrast, the correlation between CA1 with both RI and DR was of similar strength ($z = 0.88$, $p = 0.38$, Steiger z-test). This suggests that although CA1 may support both RI and DR, DG more strongly supports RI.

Finally, we tested relationships between pathology and MTL sub-regional volumes (Figure 1). Within the hippocampus, all three AD-specific biomarkers (i.e., FBP SUVR, CSF $A\beta_{42}/A\beta_{40}$, and CSF p-tau) were associated with decreased volume in CA1 and subiculum (p's < 0.05; Table S1), but not in DG or CA3. In the cortex, higher FBP SUVR was additionally associated with decreased BA35 volume ($r = -0.41$, $p = 0.03$). CSF p-tau demonstrated trend-level associations with decreased BA35 and EC volume ($0.05 < p$'s < 0.062). Although no significant associations emerged with t-tau, there was a trend-level relationship with decreased BA35 volume ($p = 0.07$).

3.3 | DG volume contributes Aβ-independent effects on retroactive interference

We next tested if considering pathology and volume together may provide more information as to the mechanisms leading to impaired RI. Based upon convergence between the previous literature on subfield contributions to RI[20] and our own volume findings, we focused on the volumes of DG and CA1. Because these regions have differential vulnerabilities to pathology, we tested how the volume of these regions in combination with pathology (i.e., FBP SUVR) predicted RI. Due to the collinearity of subfield volumes, we constructed separate stepwise linear regression models for each subfield. As a first step, we included demographic variables (age, sex, education; Model 1), then added FBP SUVR (Model 2) to determine the role of pathology, and finally added either DG (Model 3A) or CA1 (Model 3B) volume to determine the role of volume.

Demographic information alone (Model 1) did not significantly predict RI (*Model Fit Measures*, Table 2). The addition of FBP SUVR (Model 2) significantly increased the overall variance explained compared to Model 1 ($\Delta R^2 = 0.23$; *Model Comparisons*, Table 2). Adding subfield volumes (Model 3A and Model 3B) also significantly increased the overall variance explained ($\Delta R^2 = 0.23/0.18$; see *Model Comparisons*, Table 2). Of interest, in Model 3A (DG), both FBP SUVR and DG volume significantly predicted RI (p's < 0.05; *Model 3A Results*, Table 2). However, in Model 3B (CA1), only CA1 volume was a significant predictor ($p = 0.006$) of RI, as FBP SUVR reduced to a trend ($p = 0.09$; *Model 3B Results*, Table 2). These results suggest that DG volume and FBP SUVR may each contribute unique variance to RI, whereas CA1 and FBP SUVR may contribute shared variance to RI.

To further explore unique and shared variance of these predictors, we conducted commonality analyses,[35] a method allowing for correlated variables to be included in the same model. We first tested the

TABLE 2 Stepwise linear regression models predicting retroactive interference.

Model fit measures		R^2	F	P
Model 1: Demographics		0.06	0.55	0.65
Model 2: Model 1 + FBP SUVR		0.29	2.71	0.05
Model 3A: Model 2 + DG volume		0.51	5.52	0.001
Model 3B: Model 2 + CA1 volume		0.47	4.58	0.004
Model Comparisons		ΔR^2	F	p
Model 1 - Model 2		0.23	8.73	0.006
Model 2 - Model 3A		0.23	12.22	0.002
Model 2 - Model 3B		0.18	8.87	0.006
Model 3A Results	**Estimate (SE)**		t	p
Intercept	−0.13 (0.50)		−0.27	0.79
Age	0.01 (0.01)		1.97	0.06
Sex	0.01 (0.06)		0.17	0.87
Education	−0.001 (0.01)		−0.07	0.95
FBP SUVR	−0.36 (0.13)		−2.71	0.01
DG Volume	605.21 (173.10)		3.50	0.002
Model 3B Results	**Estimate (SE)**		t	p
Intercept	−0.56 (0.65)		−0.86	0.40
Age	0.01 (0.01)		2.21	0.04
Sex	0.04 (0.06)		0.63	0.53
Education	0.01 (0.01)		0.52	0.61
FBP SUVR	−0.26 (0.15)		−1.74	0.09
CA1 Volume	387.15 (129.98)		2.98	0.006

Note: Demographics include age, sex, and education.
Abbreviations: DG, dentate gyrus; FBP, ^{18}F-florbetapir PET (positron emission tomography); SE, standard error; SUVR, standardized uptake value ratio.

effect of CA1 volume and DG volume in the same model, predicting to RI (Analysis 1; Table 3). Approximately 66.3% of the variance of RI was common to CA1 volume and DG volume, whereas CA1 volume contributed 20.3% unique variance and DG volume contributed 13.4% unique variance. In contrast, in a model predicting to DR, the unique variance of CA1 volume was the strongest predictor (71.9%), whereas unique variance of DG volume was minimal (2.8%). We next tested unique and shared variance of CA1 volume, DG volume, and FBP SUVR in predicting RI (Analysis 2; Table 3). In this model, the strongest total effects were common variance between CA1 volume and DG volume (33.0%) and common variance to all three predictors (22.7%). With the addition of FBP SUVR, the unique variance explained by CA1 volume reduced to 4.7%, whereas the unique variance explained by DG volume remained similar (14.4%). In the model predicting to DR, DG volume did not strongly contribute unique variance (0.7%), whereas common variance between CA1 volume and FBP SUVR explained the most variance (31.7%). These results further support the stronger role of DG volume in RI compared to DR, and the contribution of shared variance of CA1 volume and FBP SUVR in predicting RI.

TABLE 3 Commonality analyses predicting retroactive interference and delayed recall.

	Retroactive interference		Delayed recall	
Analysis 1	**Coefficient**	**% Total**	**Coefficient**	**% Total**
Unique to CA1 vol	0.09	20.3%	0.18	71.9%
Unique to DG vol	0.06	13.4%	0.01	2.8%
Common to CA1 vol & DG vol	0.28	66.3%	0.06	25.3%
Analysis 2	**Coefficient**	**% Total**	**Coefficient**	**% Total**
Unique to CA1 vol	0.02	4.7%	0.08	22.1%
Unique to DG vol	0.07	14.4%	0.003	0.7%
Unique to FBP SUVR	0.08	16.1%	0.09	25.1%
Common to CA1 vol & DG vol	0.17	33.0%	0.03	7.7%
Common to CA1 vol & FBP SUVR	0.06	12.3%	0.11	31.7%
Common to DG vol & FBP SUVR	−0.02	−3.2%	0.005	1.4%
Common to CA1 vol & DG vol & FBP SUVR	0.12	22.7%	0.04	11.2%

Note: Analysis 1 included CA1 volume and DG volume as predictors of retroactive interference and delayed recall. Analysis 2 included CA1 volume, DG volume, and FBP SUVR as predictors of retroactive interference and delayed recall.

3.4 | CA1 volume mediates the relationship between AD pathology and retroactive interference

To further test the potential shared variance of CA1 volume and pathology on RI, we next constructed mediation models to determine if CA1 volume mediated the relationship between pathology and RI. These mediation models were valid to construct because all variables included were significantly correlated with each other (p's < 0.05, see Figure 2A-E). DG volume was not associated with FBP SUVR; therefore, we were not able to construct mediation models.

In the first mediation model, we tested whether CA1 volume mediated the relationship between FBP SUVR and RI (Figure 2F). In Step 1, the effect of FBP SUVR on RI was significant ($\beta = -0.45, p = 0.006$; path c). In Step 2, the effect of FBP SUVR on CA1 volume was significant ($\beta = -0.50, p = 0.02$; path a). In Step 3, the effect of CA1 volume on RI, while controlling for FBP SUVR, was significant ($\beta = 0.39, p = 0.006$; path b). The ACME, or the indirect effect of FBP SUVR on RI that goes through CA1 volume, was significant ($\beta = -0.19$, CI [−0.43, −0.03], $p = 0.01$; path ab). In contrast, the Average Direct Effect (ADE), or the effect of FBP SUVR on RI controlling for CA1 volume, was not significant, as the CI crossed zero ($\beta = -0.26$, CI [−0.56, 0.04], $p = 0.09$; path c'). These results suggest that CA1 volume fully mediates the relationship between FBP SUVR and RI.

In the second mediation model, we tested whether CA1 volume mediated the relationship between p-tau and RI (Figure 2G). In Step 1, the effect of p-tau on RI was significant ($\beta = -0.006, p = 0.02$; path c). In Step 2, the effect of p-tau on CA1 volume was significant ($\beta = -0.006, p = 0.04$; path a). In Step 3, the effect of CA1 volume on RI, while controlling for p-tau, was significant ($\beta = 0.49, p = 0.001$; path b). The ACME, or the indirect effect of p-tau on RI that goes through CA1 volume, was significant ($\beta = -0.003$, CI [−0.007, 0.00], $p = 0.03$). In contrast, the ADE, or the effect of p-tau on RI controlling for CA1 volume, was not significant ($\beta = -0.003$, CI [−0.007, 0.00], $p = 0.21$).

These results suggest that CA1 volume also fully mediates the relationship between p-tau and RI.

As an alternative analysis, we next repeated the mediation models predicting to DR instead of RI. The mediations of FBP SUVR/p-tau and DR by CA1 volume had CIs including zero, indicating a lack of a significant effect (FBP SUVR: ACME $\beta = -0.03$, CI [−0.08, 0.00], $p = 0.07$; p-tau: ACME $\beta = -0.04$, CI [−0.10, 0.00], $p = 0.054$). Alternative models predicting to memory using volume of BA35 or subiculum as the mediator (chosen based upon significant bivariate correlations with both memory and pathology) were not significant, as the CI crossed zero (BA35 mediating FBP and RI: ACME $\beta = -0.08$, CI [−0.26, 0.06], $p = 0.28$; subiculum mediating p-tau and DR: ACME $\beta = -0.04$, CI [−0.10, 0.01], $p = 0.11$). Overall, these non-significant alternative mediation models support the specificity of CA1 in facilitating the relationship between the AD pathology and RI.

4 | DISCUSSION

Our findings provide insights into the pathological and neurodegenerative mechanisms that lead to subtle memory impairment in aging and preclinical AD. We demonstrate that RI, a measure of interference during memory consolidation[17] thought to be sensitive to hippocampal function,[18–20] has strong associations with both PET and CSF biomarkers of AD pathology, as well as volume within specific hippocampal subfields. We further demonstrate that DG volume contributes unique variance to RI that is not explained by pathological load, whereas CA1 volume mediates the relationship between AD pathology and RI. Our findings highlight the specificity of different hippocampal subfields to pathology and memory performance and suggest a neurodegenerative-mediated pathway between pathology and memory deficits in cognitively normal older adults.
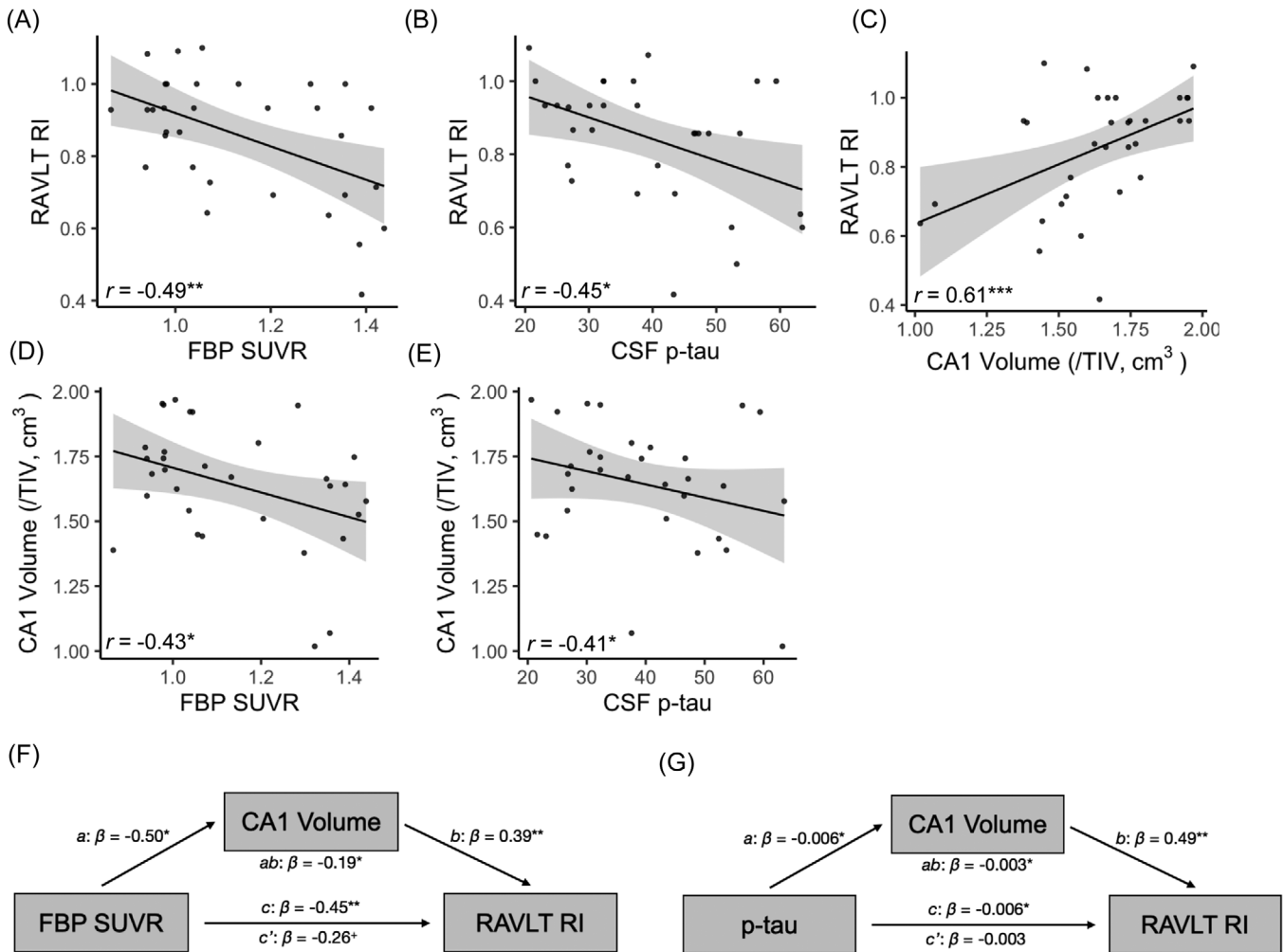
FIGURE 2 CA1 volume mediates the relationship between Alzheimer's pathology and retroactive interference (RI). Partial correlations between variables included in mediation models are shown in A-E (visualization of associations from Figure 1). All correlations were significant, making them eligible for inclusion in the mediation models. CA1 volume fully mediated the relationship between FBP SUVR and RI (F) as well as the relationship between p-tau and RI (G), indicated by the Average Casual Mediation Effect (path *ab*). ***$p < 0.001$ **$p < 0.01$ *$p < 0.05$ +$p < 0.10$. RI, retroactive interference; FBP SUVR, 18F-florbetapir-PET.

Our aim was to elucidate mechanisms of memory decline in aging and preclinical AD by testing relationships between memory, pathology, and MTL subregional volume. It has long been established through ex vivo investigations that specific MTL subregions—specifically transentorhinal/entorhinal cortex, CA1, and subiculum—are more vulnerable to the development of tau pathology and prone to early neurodegeneration, whereas regions such as DG and CA3 are resistant to the effects of pathology until later stages of AD.[2,37–39] Advances in MRI-based segmentations have enabled in vivo examination of these effects, replicating this regional vulnerability across the spectrum of aging and AD.[10,12,13,29,40–48]

Previous in vivo research within cognitively normal samples have examined relationships between AD pathology and anterior/posterior hippocampal segments,[12,13,49] or assessed hippocampal subfield volume using scans with lower than ideal resolution for subfield measurement[50] and/or less reliable automated software[51] based upon T1-weighted images.[14,52–56] To our knowledge, our study is among the

first to examine relationships between AD pathology biomarkers with hippocampal subfield volumes derived from T2-weighted structural images with sufficiently high in-plane resolution (0.4 mm × 0.4 mm) processed with validated automated techniques[29] to enable more accurate subfield delineation.[50] Our findings extend previous work by demonstrating strong associations between AD pathology biomarkers (Aβ-PET, CSF Aβ_{42}/Aβ_{40}, and CSF p-tau) and volumes of CA1, subiculum, and transentorhinal cortex/BA35, consistent with ex vivo work, suggesting that these regions are highly vulnerable to pathology. Our work parallels findings from recent studies demonstrating preferential relationships between AD pathology and volume of CA1 and subiculum in nondemented older adults,[14,53–56] consistent with findings that CA1 and subiculum atrophy best predicts transition from cognitively normal to mild cognitive impairment (MCI).[46] We did not observe a direct association between pathology and DG or CA3 volume, consistent with resistance to local pathology in these regions.[2] However, neurodegeneration in the DG and CA3 may still result from pathology

accumulation within the entorhinal cortex, which disconnects DG/CA3 from receiving normal input through the perforant pathway.[22,57]

In addition to pathology-volume associations, we closely examined how these factors together contribute to memory impairment. A novel approach in our current study is our focus on a more granular measure of memory performance, RI, which is a hippocampal-dependent process[18-20] that reflects the ability to consolidate relevant information in memory while ignoring distractors.[17] Traditional measures of word-list learning, such as DR, do not specifically isolate the mechanisms that lead to forgetting. We demonstrate that both AD pathology (i.e., FBP-PET, CSF $A\beta_{42}/A\beta_{40}$, CSF p-tau) and neurodegeneration within MTL subregions (e.g. DG, CA1) are closely associated with RI, suggesting that RI may be more sensitive to subtle hippocampal dysfunction. Previous studies in older adults using similar measures of interference during word-list learning have also demonstrated associations with pathology[7] and anterolateral EC volume,[58] but had not investigated contributions of hippocampal subfields to RI. We demonstrate that volumes of DG and CA3 are strongly associated with RI, but not DR. This suggests that RI, reflecting resistance to interference rather than non-specific mechanisms of forgetting, may be a sensitive marker of DG/CA3 dysfunction. This finding is consistent with previous work demonstrating DG/CA3's specific and critical role in orthogonalization of non-overlapping stimuli during pattern separation.[21,22]

Our findings support a distinction between DG and CA1 in the cascade between pathology accumulation and memory impairment. We found that DG volume and $A\beta$ pathology each contribute unique variance to memory performance, suggesting that the contributions of DG volume to memory performance may be independent of pathology. This is consistent with previous findings in animal models that suggest that DG is particularly vulnerable to non–pathology-related changes in aging such as decreased inhibition in the hilar region[59] and loss of reelin protein.[60] In contrast, CA1 volume fully meditated the relationship between both $A\beta$ and p-tau pathology with RI, suggesting that CA1 volume may be a specific neurodegenerative marker for predicting memory deficits in preclinical AD. Our finding extends previous work demonstrating that presubiculum volume links tau pathology and delayed recall[53] by also implicating CA1 volume, further supporting the vulnerability of CA1 to pathology.[2]

Limitations of the current study include the relatively small sample size and the reduced power, which may have resulted in alternative models not reaching statistical significance. Future research in larger samples that more accurately represent the diverse aging population may uncover additional relationships between pathology, volume, and memory. In addition, there was variation in time between CSF and PET/MRI/memory measurements; however, this was controlled for in all analyses and was not related to demographic factors. Future research should investigate longitudinal changes in these relationships, which may be more sensitive[10,12,13] and further clarify directionality. A longitudinal design would also overcome the confound of individual differences contributing to our interpretation of disease mechanisms.

In summary, we demonstrate that MTL subregions have distinct relationships with episodic memory domains and AD pathology in non-demented older adults. DG volume was specifically associated with RI but not related to AD pathology, suggesting AD pathology-independent effects on memory. In contrast, CA1 volume fully mediated the relationship between AD pathology and RI. Overall, RI may be a more sensitive marker of subtle cognitive impairment than delayed recall, reflecting both AD pathology and hippocampal subfield integrity, and may provide benefit as an outcome measure in clinical trials.

CONFLICTS OF INTEREST STATEMENT

Michael A. Yassa is Co-founder and Chief Scientific Officer of Augnition Labs, LLC. No other authors have conflicts of interest or disclosures. Author disclosures are available in the supporting information.

ORCID

Jenna N. Adams https://orcid.org/0000-0002-6702-3851

REFERENCES

1. Jack CR, Bennett DA, Blennow K, et al. NIA-AA research framework: toward a biological definition of Alzheimer's disease. *Alzheimers Dement*. 2018;14:535-562.
2. Braak H, Braak E. Neuropathological stageing of Alzheimer-related changes. *Acta Neuropathol*. 1991;82:239-259.
3. Jack CR, Knopman DS, Jagust WJ, et al. Hypothetical model of dynamic biomarkers of the Alzheimer's pathological cascade. *Lancet Neurol*. 2010;9:119-128.
4. Schöll M, Maass A, Mattsson N, et al. Biomarkers for tau pathology. *Mol Cell Neurosci*. 2019;97:18-33. doi:10.1016/J.MCN.2018.12.001
5. Strozyk D, Blennow K, White LR, Launer LJ. CSF Aß 42 levels correlate with amyloid-neuropathology in a population-based autopsy study. *Neurology*. 2003;60:652-656.
6. Blennow K, Zetterberg H. Biomarkers for Alzheimer's disease: current status and prospects for the future. *J Intern Med*. 2018;284:643-663.
7. Yeung LK, Hale C, Last BS, et al. Cerebrospinal fluid amyloid levels are associated with delayed memory retention in cognitively normal biomarker-negative older adults. *Neurobiol Aging*. 2019;84:90-97.
8. Maass A, Lockhart SN, Harrison TM, et al. Entorhinal tau pathology, episodic memory decline and neurodegeneration in aging. *J Neurosci*. 2017;38(3):530-543. doi:10.1523/JNEUROSCI.2028-17.2017
9. Squire LR, Zola-Morgan S. The medial temporal lobe memory system. *Science*. 1991;253:1380-1386.
10. Das SR, Xie L, Wisse LEM, et al. Longitudinal and cross-sectional structural magnetic resonance imaging correlates of AV-1451 uptake. *Neurobiol Aging*. 2018;66:49-58.
11. LaPoint MR, Chhatwal JP, Sepulcre J, Johnson KA, Sperling RA, Schultz AP. The association between tau PET and retrospective cortical thinning in clinically normal elderly. *Neuroimage*. 2017;157:612-622.
12. Wisse LE, Xie L, Das SR, et al. Tau pathology mediates age effects on medial temporal lobe structure. *Neurobiol Aging*. 2022;109:135-144.

13. Xie L, Wisse LEM, Das SR, et al. Longitudinal atrophy in early Braak regions in preclinical Alzheimer's disease. *Hum Brain Mapp.* 2020;41:4704-4717.

14. Parker TD, Cash DM, Lane CAS, et al. Hippocampal subfield volumes and preclinical Alzheimer's disease in 408 cognitively normal adults born in 1946. *PLoS One.* 2019;14:e0224030.

15. Wisse LEM, Ravikumar S, Ittyerah R, et al. Downstream effects of poly-pathology on neurodegeneration of medial temporal lobe subregions. *Acta Neuropathol Commun.* 2021;9:128.

16. Mormino EC, Kluth JT, Madison CM, et al. Episodic memory loss is related to hippocampal-mediated β-amyloid deposition in elderly subjects. *Brain.* 2009;132:1310-1323.

17. Wixted JT. On common ground: jost's (1897) law of forgetting and Ribot's (1881) law of retrograde amnesia. *Psychol Rev.* 2004;111:864-879.

18. Villar ME, Martinez MC, Lopes da Cunha P, Ballarini F, Viola H. Memory consolidation and expression of object recognition are susceptible to retroactive interference. *Neurobiol Learn Mem.* 2017;138:198-205.

19. Lillywhite LM, Saling MM, Briellmann RS, Weintrob DL, Pell GS, Jackson GD. Differential contributions of the hippocampus and rhinal cortices to verbal memory in epilepsy. *Epilepsy Behav.* 2007;10:553-559.

20. Martínez MC, Villar ME, Ballarini F, Viola H. Retroactive interference of object-in-context long-term memory: role of dorsal hippocampus and medial prefrontal cortex. *Hippocampus.* 2014;24:1482-1492.

21. Wilson IA, Gallagher M, Eichenbaum H, Tanila H. Neurocognitive aging: prior memories hinder new hippocampal encoding. *Trends Neurosci.* 2006;29:662-670.

22. Leal SL, Yassa MA. Integrating new findings and examining clinical applications of pattern separation. *Nat Neurosci.* 2018;21:163-173.

23. Tombaugh TN, McIntyre NJ. The Mini-Mental State Examination. *Prog Geriatr.* 1992;40:922-935.

24. Schmidt M. *Rey auditory verbal learning test: a handbook.* Western Psychological Services; 1996.

25. Alcolea D, Pegueroles J, Muñoz L, et al. Agreement of amyloid PET and CSF biomarkers for Alzheimer's disease on Lumipulse. *Ann Clin Transl Neurol.* 2019;6:1815-1824.

26. Landau SM, Mintun MA, Joshi AD, et al. Amyloid deposition, hypometabolism, and longitudinal cognitive decline. *Ann Neurol.* 2012;72:578-586.

27. Landau SM, Breault C, Joshi AD, et al. Amyloid-β imaging with Pittsburgh compound B and florbetapir: comparing radiotracers and quantification methods. *J Nucl Med.* 2013;54:70-77.

28. Fischl B. FreeSurfer. *Neuroimage.* 2012;62:774-781.

29. Yushkevich PA, Pluta JB, Wang H, et al. Automated volumetry and regional thickness analysis of hippocampal subfields and medial temporal cortical structures in mild cognitive impairment. *Hum Brain Mapp.* 2015;36:258-287.

30. Tustison NJ, Cook PA, Holbrook AJ, et al. The ANTsX ecosystem for quantitative biological and medical imaging. *Sci Rep.* 2021;11:9068.

31. Keshavan A, Wellington H, Chen Z, et al. Concordance of CSF measures of alzheimer's pathology with amyloid pet status in a preclinical cohort: a comparison of lumipulse and established immunoassays. *Alzheimers Dement (Amst).* 2021;13:e12131.

32. Campbell MR, Ashrafzadeh-Kian S, Petersen RC, et al. P-tau/aβ42 and aβ42/40 ratios in csf are equally predictive of amyloid pet status. *Alzheimers Dement (Amst).* 2021;13:e12190.

33. Willemse EAJ, Tijms BM, van Berckel BNM, et al. Comparing CSF amyloid-beta biomarker ratios for two automated immunoassays, elecsys and lumipulse, with amyloid pet status. *Alzheimers Dement (Amst).* 2021;13:e12182.

34. Steiger JH. Tests for comparing elements of a correlation matrix. *Psychol Bull.* 1980;87:245-251.

35. Lindenberger U, Pötter U. The complex nature of unique and shared effects in hierarchical linear regression: implications for developmental psychology. *Psychol Methods.* 1998;3:218-230.

36. Tingley D, Yamamoto T, Hirose K, Keele L, Imai K. Mediation: r package for causal mediation analysis. *J Stat Softw.* 2014;59:1-38.

37. Šimić G, Kostović I, Winblad B, Bogdanović N. Volume and number of neurons of the human hippocampal formation in normal aging and Alzheimer's disease. *J Comp Neurol.* 1997;379:482-494.

38. West MJ, Coleman PD, Flood DG, Troncoso JC. Differences in the pattern of hippocampal neuronal loss in normal ageing and Alzheimer's disease. *Lancet.* 1994;344:769-772.

39. Bobinski M, Wegiel J, Tarnawski M, et al. Relationships between regional neuronal loss and neurofibrillary changes in the hippocampal formation and duration and severity of Alzheimer disease. *J Neuropathol Exp Neurol.* 1997;56:414-420.

40. Wolk DA, Das SR, Mueller SG, Weiner MW, Yushkevich PA. Medial temporal lobe subregional morphometry using high resolution MRI in Alzheimer's disease. *Neurobiol Aging.* 2017;49:204-213.

41. Mueller SG, Schuff N, Yaffe K, Madison C, Miller B, Weiner MW. Hippocampal atrophy patterns in mild cognitive impairment and alzheimer's disease. *Hum Brain Mapp.* 2010;31:1339-1347.

42. Csernansky JG, Wang L, Joshi S, et al. Early DAT is distinguished from aging by high-dimensional mapping of the hippocampus. *Neurology.* 2000;55:1636-1643.

43. de Flores R, La Joie R, Chételat G. Structural imaging of hippocampal subfields in healthy aging and Alzheimer's disease. *Neuroscience.* 2015;309:29-50.

44. Thompson PM, Hayashi KM, De Zubicaray GI, et al. Mapping hippocampal and ventricular change in Alzheimer disease. *Neuroimage.* 2004;22:1754-1766.

45. La Joie R, Perrotin A, de La Sayette V, et al. Hippocampal subfield volumetry in mild cognitive impairment, Alzheimer's disease and semantic dementia. *NeuroImage Clin.* 2013;3:155-162.

46. Apostolova LG, Mosconi L, Thompson PM, et al. Subregional hippocampal atrophy predicts Alzheimer's dementia in the cognitively normal. *Neurobiol Aging.* 2010;1:1077-1088.

47. Apostolova LG, Zarow C, Biado K, et al. Relationship between hippocampal atrophy and neuropathology markers: a 7T MRI validation study of the EADC-ADNI harmonized hippocampal segmentation protocol. *Alzheimers Dement.* 2015;11:139-150.

48. Wisse LEM, Biessels GJ, Heringa SM, et al. Hippocampal subfield volumes at 7T in early Alzheimer's disease and normal aging. *Neurobiol Aging.* 2014;35:2039-2045.

49. Berron D, Vogel JW, Insel PS, et al. Early stages of tau pathology and its associations with functional connectivity, atrophy and memory. *Brain.* 2021;144(9):2771-2783. doi:10.1093/brain/awab114

50. Wisse LEM, Chételat G, Daugherty AM, et al. Hippocampal subfield volumetry from structural isotropic 1 mm3 MRI scans: a note of caution. *Hum Brain Mapp.* 2021;42:539-550.

51. Wisse L, Biessels G, Geerlings M. A critical appraisal of the hippocampal subfield segmentation package in FreeSurfer. *Front Aging Neurosci.* 2014;6:261.

52. Müller-Ehrenberg L, Riphagen JM, Verhey FRJ, Sack AT, Jacobs HIL. Alzheimer's disease biomarkers have distinct associations with specific hippocampal subfield volumes. *J Alzheimer's Dis.* 2018;66:811-823.

53. Jacobs HIL, Augustinack JC, Schultz AP, et al. The presubiculum links incipient amyloid and tau pathology to memory function in older persons. *Neurology.* 2020;94:e1916-e1928.

54. Zhang L, Mak E, Reilhac A, et al. Longitudinal trajectory of amyloid-related hippocampal subfield atrophy in nondemented elderly. *Hum Brain Mapp.* 2020;41:2037-2047.

55. Hsu PJ, Shou H, Benzinger T, et al. Amyloid burden in cognitively normal elderly is associated with preferential hippocampal subfield volume loss. *J Alzheimer's Dis.* 2015;45:27-33.

56. Kagerer SM, Schroeder C, van Bergen JMG, et al. Low subicular volume as an indicator of dementia-risk susceptibility in old age. *Front Aging Neurosci.* 2022;14:1-13.

57. Hyman BT, Van Hoesen GW, Damasio AR, Barnes CL. Alzheimer's disease : cell-specific pathology isolates the hippocampal formation. *Science.* 1984;225:1168-1170.
58. Yeung LK, Hale C, Rizvi B, et al. Anterolateral entorhinal cortex volume is associated with memory retention in clinically unimpaired older adults. *Neurobiol Aging.* 2021;98:134-145.
59. Spiegel AM, Koh MT, Vogt NM, Rapp PR, Gallagher M. Hilar interneuron vulnerability distinguishes aged rats with memory impairment. *J Comp Neurol.* 2013;521:3508-3523.
60. Stranahan AM, Haberman RP, Gallagher M. Cognitive decline is associated with reduced reelin expression in the entorhinal cortex of aged rats. *Cereb Cortex.* 2011;21:392-400.

SUPPORTING INFORMATION

Additional supporting information can be found online in the Supporting Information section at the end of this article.